Abstract

Measurement of total hadronic differential cross sections in the LArIAT experiment

Elena Gramellini

2018

Abstract goes here. Limit 750 words.

Measurement of total hadronic differential cross sections in the LArIAT experiment

A Dissertation
Presented to the Faculty of the Graduate School
of
Yale University
in Candidacy for the Degree of
Doctor of Philosophy

by
Elena Gramellini

Dissertation Director: Bonnie T. Fleming

Date you'll receive your degree

A mia mamma e mio babbo,

grazie per le radici e grazie per le ali.

To my mom and dad,

thank you for the roots and thank you for the wings.

Contents

Acknowledgements

"*Dunque io ringrazio tutti quanti.*
Specie la mia mamma che mi ha fatto cosí funky."
– Articolo 31, Tanqi Funky, 1996 –

"*At last, I thank everyone.*
Especially my mom who made me so funky."
– Articolo 31, Tanqi Funky, 1996 –

A lot of people are awesome, especially you, since you probably agreed to read this when it was a draft.

Chapter 0

Total Ha(π^-,Ar)dronic Cross Section Measurement Methodology

This chapter describes the general procedure employed to measure a total hadronic differential cross section in LArIAT. Albeit with small differences, both the (π^-,Ar) and (K^+,Ar) total hadronic cross section measurements rely on the same procedure described in details in the following sections. We start by selecting the particle of interest using a combination of beamline detectors and TPC information (Section 0.1). We then perform a handshake between the beamline information and the TPC tracking to assure the selection of the right TPC track (Section 0.2). Finally, we apply the "thin slice" method and measure the "raw" hadronic cross section (Section 0.3). A series of corrections are then evaluated to obtain the "true" cross section (Section 0.3.3).

At the end of this chapter, we show a sanity check of the methodology against MC truth information (Section 0.4).

0.1 Event Selection

The measurement of the (π^-,Ar) and (K^+,Ar) total hadronic cross section in LArIAT starts by selecting the pool of pion or kaon candidates and measuring their momentum. This is done through the series of selections on beamline and TPC information described in the next sections. The summary of the event selection in data is reported in Table 1.

Selection of Beamline Events

As shown in equation 5, we leverage the beamline particle identification and momentum measurement before entering the TPC as in input to evaluate the kinetic energy for the hadrons used in the cross sections measurements. Thus, we select the LArIAT data to keep only events whose wire chamber and time of flight information is registered (line 2 in in Table 1). Additionally, we perform a check of the plausibility of the trajectory inside the beamline detectors: given the position of the hits in the four wire chambers, we make sure the particle's trajectory does not cross any impenetrable material such as the collimator and the magnets steel (line 3 in in Table 1).

	Run-II Negative Polarity	Run-II Positive Polarity
Events Reconstructed in Beamline	158396	260810
Events with Plausible Trajectory	147468	240954
Beamline $\pi^-/\mu^-/e^-$ Candidate	138481	N.A.
Beamline K^+ Candidate	N.A	2837
Events Surviving Pile Up Filter	108929	2389
Events with WC2TPC Match	41757	1081
Events Surviving Shower Filter	40841	N.A.
Available Events For Cross Section	40841	1081

Table 1: Number of data events for Run-II Negative and Positive polarity

Particle Identification in the beamline

In data, the main tool to establish the identity of the hadron of interest is the LArIAT tertiary beamline, in its function of mass spectrometer. We combine the measurement of the time of flight, TOF, and the beamline momentum, p_{Beam}, to reconstruct the invariant mass of the particles in the beamline, m_{Beam}, as follows

$$m_{Beam} = \frac{p_{Beam}}{c}\sqrt{\left(\frac{TOF * c}{l}\right)^2 - 1}, \tag{1}$$

where c is the speed of light and l is the length of the particle's trajectory between the time of flight paddels.

Figure 1 shows the mass distribution for the Run II negative polarity runs on the left and positive polarity runs on the right. We perform the classification of events into the different samples as follows:

- $\underline{\pi/\mu/e}$: mass $<$ 350 MeV
- <u>kaon:</u> 350 MeV $<$ mass $<$ 650 MeV
- <u>proton:</u> 650 MeV $<$ mass $<$ 3000 MeV.

Lines 4 and 5 in in Table 1 show the number of negative $\pi/\mu/e$ and positive K candidates which pass the mass selection for LArIAT Run-II data.

TPC Selection: Halo mitigation

The secondary beam impinging on LArIAT secondary target produces a plethora of particles which propagates downstream. The presence of upstream and downstream collimators greatly abates the number of particles tracing down the LArIAT tertiary beamline. However, it is possible that more than one particle sneaks into the LArTPC during its readout time: the TPC readout is triggered by the particle firing the

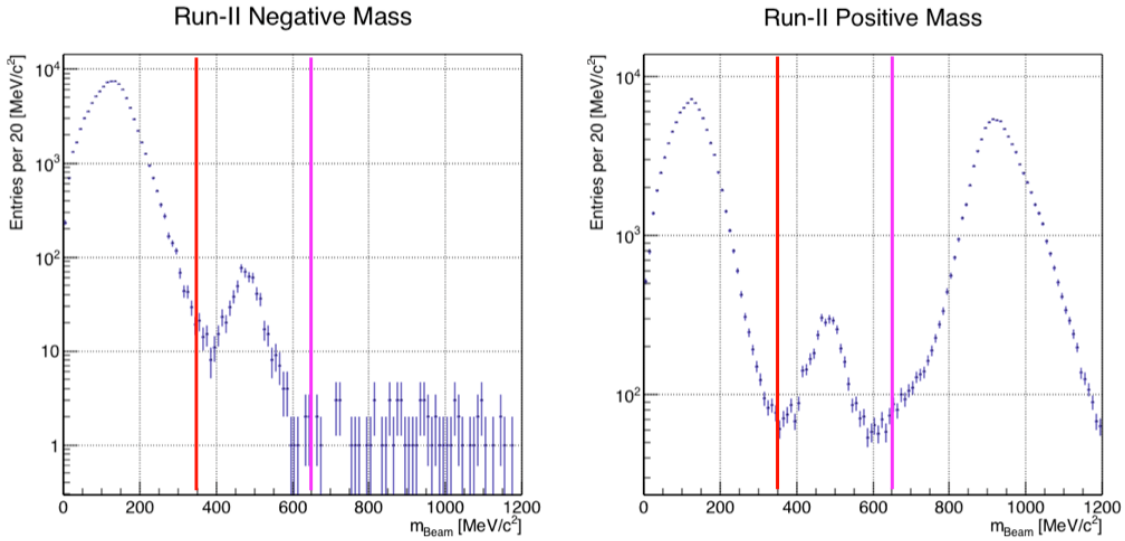

Figure 1: Distribution of the beamline mass as calculated according to equation 1 for the Run-II events reconstructed in the beamline, negative polarity runs on the left and positive polarity runs on the right. The classification of the events into $\pi^{\pm}/\mu^{\pm}/e^{\pm}$, $K^{\pm}$, or (anti)proton is based on these distributions, whose selection cut are represented by the vertical colored lines.

beamline detectors, but particles from the beam halo might be present in the TPC at the same time. We call "pile up" the additional traces in the TPC. We adjusted the primary beam intensity between LArIAT Run I and Run II to reduce the presence of events with high pile up particles in the data sample. For the cross section analyses, we remove events with more than 4 tracks in the first 14 cm upstream portion of the TPC from the sample (line 6 in in Table 1).

TPC Selection: Shower Removal

In the case of the (π^-,Ar) cross section, the resolution of beamline mass spectrometer is not sufficient to select a beam of pure pions. In fact, muons and electrons survive the selection on the beamline mass. It is important to notice that the composition of the negative polarity beam is mostly pions, as will be discussed in section 1.1.1. Anyhow, we devise a selection on the TPC information to mitigate the presence of

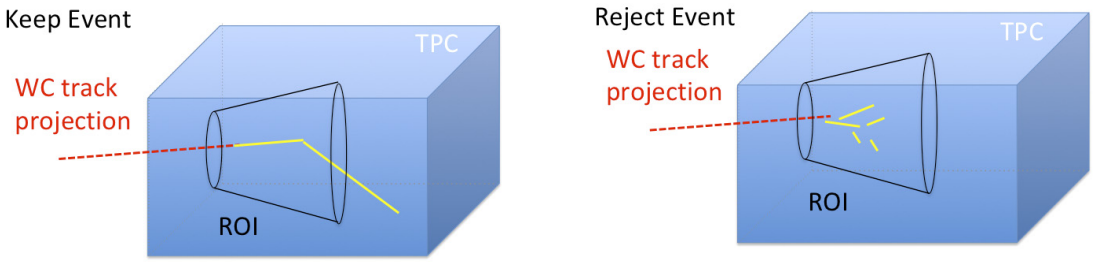

Figure 2: Visual rendering of the shower filter. The ROI is a cut cone, with a small radius of 4 cm, a big radius of 10 cm and an height of 42 cm (corresponding to 3 radiation lengths for electrons in Argon).

electrons in the sample used for the pion cross section. The selection relies on the different topologies of a pion and an electron event in the argon: while the former will trace a track inside the TPC active volume, the latter will tend to "shower", i.e. interact with the medium, producing bremsstrahlung photons which pair convert into several short tracks. In order to remove the shower topology, we create a region of interest (ROI) around the TPC track corresponding to the beamline particle (more details on this in the next section). We look for short tracks contained in the ROI, as depicted in figure 4: if more then 5 tracks shorter than 10 cm are in the ROI, we reject the event. Line 8 in in Table 1) shows the number of events surviving this selection.

0.2 Beamline and TPC Handshake: the Wire Chamber to TPC Match

For each event passing the selection on its beamline information, we need to identify the track inside the TPC corresponding to the particle which triggered the beamline detectors, a procedure we refer to as "WC to TPC match" (WC2TPC for short). In general, the TPC tracking algorithm will reconstruct more than one track in the event, partially due to the fact that hadrons interact in the chamber and partially

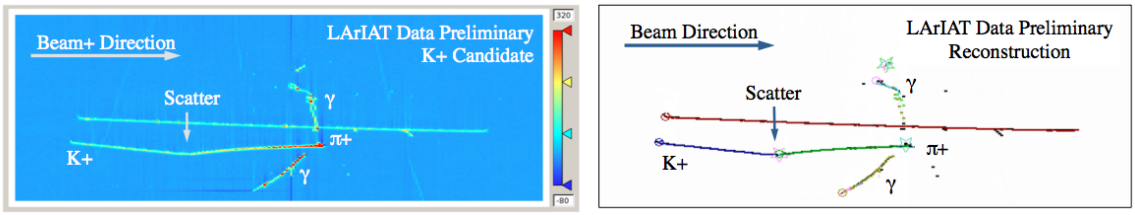

Figure 3: Kaon candidate event: on the right, event display showing raw quantities; on the left, event display showing reconstructed tracks. In the reconstructed event display, different colors represent different track objects. A kink is visible in the kaon ionization, signature of a hadronic interaction: the tracking correctly stops at the kink position and two tracks are formed. An additional pile-up track is so present in the event (top track).

because of pile up particles during the triggered TPC readout time, as shown in figure 3.

We attempt to uniquely match one wire chamber track to one and only one reconstructed TPC track. In order to determine if the presence of a match, we apply a geometrical selection on the relative the position of the wire chamber and TPC tracks. We start by considering only TPC tracks whose first point is in the first 2 cm upstream portion of the TPC for the match. We project the wire chamber track to the TPC front face where we define the coordinates of the projected point as x_{FF} and y_{FF}. For each considered TPC track, we define ΔX as the difference between the x position of the most upstream point of the TPC track and x_{FF}. ΔY is defined analogously. We define the radius difference, ΔR, as $\Delta \mathrm{R} = \sqrt{\Delta \mathrm{X}^2 + \Delta \mathrm{Y}^2}$. We define as α the angle between the incident WC track and the TPC track in the plane that contains them. If $\Delta \mathrm{R} < 4$ cm, $\alpha < 8°$, a match between WC-track and TPC reconstructed track is found. We describe how we determine the value for the radius and angular selection in sec 1.2.1. In MC, we mimic the matching between the WC and the TPC track by constructing a fake WC track using truth information at wire chamber four. We then apply the same WC to TPC matching algorithm as in data. We discard events with multiple WC2TPC matches. We use only those TPC tracks that are matched to WC tracks in the cross section calculation.

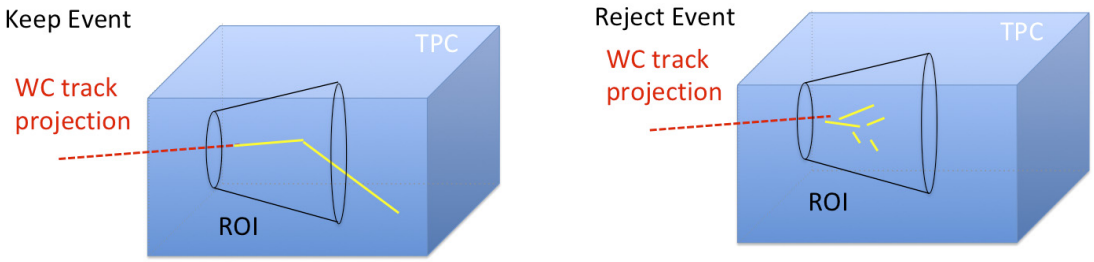

Figure 4: Visual rendering of the wire chamber to TPC match.

0.3 The Thin Slice Method

Once we have selected the pool of hadron candidates and we have identified the TPC track corresponding to the beamline event, we apply the thin slice method to measure the cross section, as the following sections describe.

0.3.1 Cross Sections on Thin Target

Cross section measurements on a thin target have been the bread and butter of nuclear and particle experimentalists since the Geiger-Marsden experiments [**?**]. At their core, these types of experiments consist in shooting a beam of particles with a known flux on a thin target and recording the outgoing flux.

In general, the target is not a single particle, but rather a slab of material containing many diffusion centers. The so-called "thin target" approximation assumes that the target centers are uniformly distributed in the material and that the target is thin compared to the projectile interaction length,WC2TPC so that no center of interaction sits in front of another. In this approximation, the ratio between the number of particles interacting in the target $N_{Interacting}$ and number of incident particles $N_{Incident}$ determines the interaction probability $P_{Interacting}$, which is the complementary to one of the survival probability $P_{Survival}$. Equation 2

$$P_{Survival} = 1 - P_{Interacting} = 1 - \frac{N_{Interacting}}{N_{Incident}} = e^{-\sigma_{TOT} n \delta X} \tag{2}$$

describes the probability for a particle to survive the thin target. This formula relates the total cross section σ_{TOT}, the density of the target centers n and the thickness of the target along the incident hadron direction δX, to the interaction probability[1]. If the target is thin compared to the interaction length of the process considered, we can Taylor expand the exponential function in equation 2 and find a simple proportionality relationship between the number of incident and interacting particles, and the cross section, as shown in equation 3:

$$1 - \frac{N_{Interacting}}{N_{Incident}} = 1 - \sigma_{TOT} n \delta X + O(\delta X^2). \tag{3}$$

Solving for the cross section, we find:

$$\sigma_{TOT} = \frac{1}{n\delta X} \frac{N_{Interacting}}{N_{Incident}}. \tag{4}$$

0.3.2 Not-so-Thin Target: Slicing the Argon

The interaction length of pions and kaons in argon is expected to be of the order of 50 cm for pions and 100 cm for kaons. Thus, the LArIAT TPC, with its 90 cm of length, is not a thin target. However, the fine-grained tracking of the LArIAT LArTPC allows us to treat the argon volume as a sequence of many adjacent thin targets.

As described in Chapter **??**, LArIAT wire planes consist of 240 wires each. The wires are oriented at +/- 60° from the vertical direction at 4 mm spacing, while the beam direction is oriented 3 degrees off the z axis in the XZ plane. The wires collect signals proportional to the energy loss of the hadron along its path in a $\delta X = 4$ mm/sin(60°) $\approx$ 4.7 mm slab of liquid argon. Thus, one can think to slice the TPC

1. The scattering center density in the target, n, relates to the argon density ρ, the Avogadro number N_A and the argon molar mass m_A as $n = \frac{\rho N_A}{m_A}$.

into many thin targets of $\delta X = 4.7$ mm thickness along the direction of the incident particle, making a measurement at each wire along the path.

Considering each slice j a "thin target", we can apply the cross section calculation from Eq. 4 iteratively, evaluating the kinetic energy of the hadron as it enters each slice, E_j^{kin}. For each WC2TPC matched particle, the energy of the hadron entering the TPC is known thanks to the momentum and mass determination by the tertiary beamline,

$$E_{FrontFace}^{kin} = \sqrt{p_{Beam}^2 - m_{Beam}^2} - m_{Beam} - E_{loss}, \tag{5}$$

where E_{loss} is a correction for the energy loss in the dead material between the beamline and the TPC front face. The energy of the hadron at each slab is determined by subtracting the energy released by the particle in the previous slabs. For example, at the j^{th} point of a track, the kinetic energy will be

$$E_j^{kin} = E_{FrontFace}^{kin} - \sum_{i<j} \Delta E_i, \tag{6}$$

where ΔE_i is the energy deposited at each argon slice before the j^{th} point as measured by the calorimetry associated with the tracking.

If the particle enters a slice, it contributes to $N_{Incident}(E^{kin})$ in the energy bin corresponding to its kinetic energy in that slice. If it interacts in the slice, it then also contributes to $N_{Interacting}(E^{kin})$ in the appropriate energy bin. The cross section as a function of kinetic energy, $\sigma_{TOT}(E^{kin})$ will then be proportional to the ratio $\frac{N_{Interacting}(E^{kin})}{N_{Incident}(E^{kin})}$.

The statistical uncertainty for each energy bin is calculated by error propagation from the statistical uncertainty on $N_{Incident}$ and $N_{Interacting}$. Since the number of incident hadrons in each energy bin is given by a simple counting, we assume that $N_{Incident}$ is distributed as a poissonian with mean and σ^2 equal to $N_{Incident}$ in each

bin. On the other hand, $N_{Interacting}$ follows a binomial distribution: a particle in a given energy bin might or might not interact. The square of the variance for the binomial is given by

$$\sigma^2 = \mathcal{N} P_{Interacting}(1 - P_{Interacting}); \tag{7}$$

since the interaction probability $P_{Interacting}$ is $\frac{N_{Interacting}}{N_{Incident}}$ and the number of tries $\mathcal{N}$ is $N_{Incident}$, equation 7 translates into

$$\sigma^2 = N_{Incident}\frac{N_{Interacting}}{N_{Incident}}(1 - \frac{N_{Interacting}}{N_{Incident}}) = N_{Interacting}(1 - \frac{N_{Interacting}}{N_{Incident}}). \tag{8}$$

$N_{Incident}$ and $N_{Interacting}$ are not independent. The uncertainty on the cross section is thus calculated as

$$\delta\sigma_{tot}(E) = \sigma_{tot}(E)\Big(\frac{\delta N_{Interacting}}{N_{Interacting}} + \frac{\delta N_{Incident}}{N_{Incident}}\Big) \tag{9}$$

where:

$$\delta N_{Incident} = \sqrt{N_{Incident}} \tag{10}$$

$$\delta N_{Interacting} = \sqrt{N_{Interacting}\Big(1 - \frac{N_{Interacting}}{N_{Incident}}\Big)}. \tag{11}$$

0.3.3 Corrections to the Raw Cross Section

Equation 4 is a prescription for measuring the cross section in case of a pure beam of the hadron of interest and 100% efficiency in the determination of the interaction point. For example, if LArIAT had a beam of pure pions and were 100% efficient in determining the interaction point within the TPC, the pion cross section in each energy bin would be given by

$$\sigma^{\pi^-}(E_i) = \frac{1}{n\delta X}\frac{N^{\pi^-}_{\text{Interacting}}(E_i)}{N^{\pi^-}_{\text{Incident}}(E_i)}. \tag{12}$$

Unfortunately, this is not the case. In fact, the selection used to isolate pions in the LArIAT beam allows for the presence of some muons and electrons as background. Also, the LArIAT TPC is not 100% efficient in determining the interaction point. Therefore we need to apply two corrections evaluated on the MC in order to extract the cross section from LArIAT data: the background subtraction and the efficiency correction. Still using the pion case as example, we estimate the pion cross section in each energy bin changing the equation 12 into

$$\sigma^{\pi^-}(E_i) = \frac{1}{n\delta X}\frac{N^{\pi^-}_{\text{Interacting}}(E_i)}{N^{\pi^-}_{\text{Incident}}(E_i)} = \frac{1}{n\delta X}\frac{\epsilon_i^{inc}[N^{\text{TOT}}_{\text{Interacting}}(E_i) - B_{\text{Interacting}}(E_i)]}{\epsilon_i^{int}[N^{\text{TOT}}_{\text{Incident}}(E_i) - B_{\text{Incident}}(E_i)]}, \quad (13)$$

where $N^{\text{TOT}}_{\text{Interacting}}(E_i)$ and $N^{\text{TOT}}_{\text{Incident}}(E_i)$ is the measured content of the interacting and incident histograms for events that pass the event selection, $B_{interacting}(E_i)$ and $B_{\text{Incident}}(E_i)$ represent the contributions from beamline background, and ϵ_i^{int} and ϵ_i^{inc} are the efficiency corrections for said histograms.

As we will show in section **??**, the background subtraction for the interacting and incident histograms can be translated into a corresponding corrections $C^{\pi MC}_{Interacting}(E_i)$ and $C^{\pi MC}_{Incident}(E_i)$ and the cross section re-written as follows

$$\sigma^{\pi^-}(E_i) = \frac{1}{n\delta X}\frac{\epsilon_i^{inc}\ N^{\text{TOT}}_{\text{Interacting}}(E_i)\ C^{\pi MC}_{Interacting}(E_i)}{\epsilon_i^{int}\ N^{\text{TOT}}_{\text{Incident}}(E_i)\ C^{\pi MC}_{Incident}(E_i)}. \quad (14)$$

0.4 Procedure testing with truth quantities

The (π^-,Ar) and (K^+,Ar) total hadronic cross section implemented in Geant4 can be used as a tool to validate the measurement methodology. We describe here a closure test done on Monte Carlo to prove that the methodology of slicing the TPC retrieves the underlying cross section distribution implemented in Geant4 within the statistical uncertainty.

For pions in the considered energy range, the Geant4 inelastic model adopted to

is "BertiniCascade", while the elastic model "hElasticLHEP". For kaons, the Geant4 inelastic model adopted to is "BertiniCascade", while the elastic model "hElasticLHEP".

For the validation test, we fire about a sample of pions and a sample of kaons inside the LArIAT TPC active volume using the Data Driven Monte Carlo (see section 1.1.2). We apply the thin-sliced method using only true quantities to calculate the hadron kinetic energy at each slab in order to decouple reconstruction effects from issues with the methodology. For each slab of 4.7 mm length along the path of the hadron, we integrate the true energy deposition as given by the Geant4 transportation model. Then, we recursively subtracted it from the hadron kinetic energy at the TPC front face to evaluate the kinetic energy at each slab until the true interaction point is reached. Since the MC is a pure beam of the hadron of interest and truth information is used to retrieve the interaction point, no correction is applied. Doing so, we obtain the true interacting and incident distributions for the considered hadron and we obtain the true MC cross section as a function of the hadron true kinetic energy.

Figure 5 shows the total hadronic cross section for argon implemented in Geant4 10.01.p3 (solid lines) overlaid with the true MC cross section as obtained with the sliced TPC method (markers) for pions on the left and kaons on the right; the total cross section is shown in green, the elastic cross section in blue and the inelastic cross section in red. The nice agreement with the Geant4 distribution and the cross section obtained with the sliced TPC method gives us confidence in the validity of the methodology.

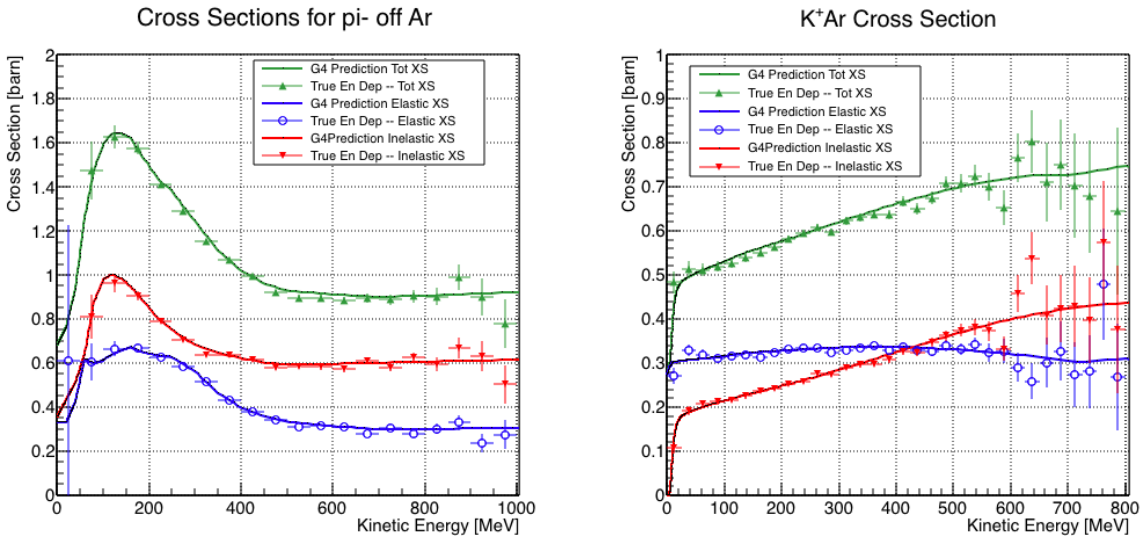

Figure 5: Hadronic cross sections for (π^-,Ar) on the left and (K^+,Ar) on the right as implemented in Geant4 10.01.p3 (solid lines) overlaid the true MC cross section as obtained with the sliced TPC method (markers). The total cross section is shown in green, the elastic cross section in blue and the inelastic cross section in red.

Chapter 1

Preparatory Work

This chapter describes the preparatory work done on the the data and Monte Carlo samples used for the cross section analyses. This entails:

1. the MC production,
2. the energy calibration of the detector both in data and MC,
3. the optimization of the tracking algorithm for the total cross section analyses.

1.1 Construction of a Monte Carlo Simulation for LArIAT

1.1.1 G4Beamline

1.1.2 Data Driven MC

1.2 Tracking Studies

1.2.1 Study of WC to TPC Match

1.3 Energy Calibration and Studies

1.4 Estimate of Energy Loss before the TPC

Chapter 2

Negative Pion Cross Section Measurement

2.1 Raw Cross Section

2.2 Background Subtracted Cross Section

2.3 Efficiency Corrected Cross Section

Chapter 3

Positive Kaon Cross Section Measurement

3.1 Raw Cross Section

Appendix A

Measurement of LArIAT Electric Field

The electric field of a LArTPC in the drift volume is a fundamental quantity for the proper functionality of this technology, as it affects almost every reconstructed quantity such as the position of hits or their collected charge. Given its importance, we calculate the electric field for LArIAT with a single line diagram from our HV circuit and we cross check the obtained value with a measurement relying only on TPC data.

Before getting into the details of the measurement procedures, it is important to explicit the relationship between some quantities in play. The electric field and the drift velocity (v_{drift}) are related as follows

$$v_{drift} = \mu(E_{field}, T)E_{field}, \tag{A.1}$$

where μ is the electron mobility, which depends on the electric field and on the temperature (T). The empirical formula for this dependency is described in [**?**] and shown in Figure A.1 for several argon temperatures.

The relationship between the drift time (t_{drift}) and the drift velocity is trivially

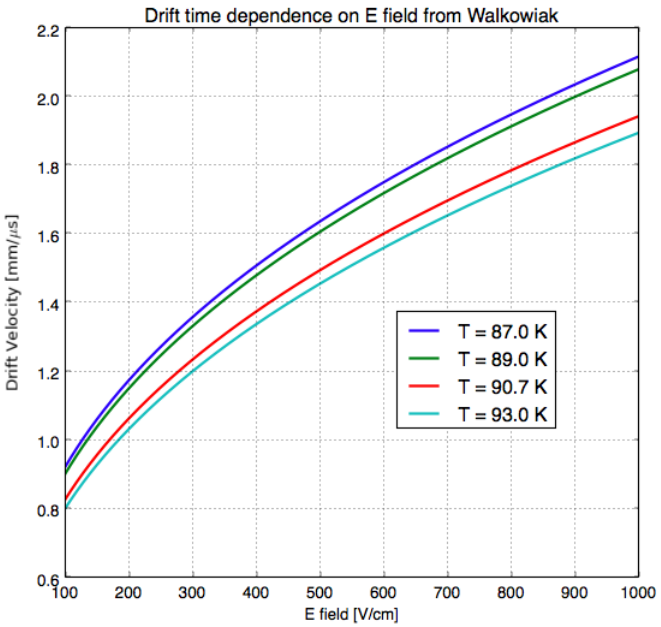

Figure A.1: Drift velocity dependence on electric field for several temperatures. The slope of the line at any one point represents the electron mobility for that given temperature and electric field.

Table A.1: Electric field and drift velocities in LArIAT smaller drift volumes

	Shield-Induction	Induction-Collection
E_{field}	700.63 V/cm	892.5 V/cm
v_{drift}	1.73 mm/μs	1.90 mm/μs
t_{drift}	2.31 μs	2.11 μs

given by

$$t_{drift} = \Delta x / v_{drift}, \tag{A.2}$$

where Δx is the distance between the edges of the drift region. Table A.1 reports the values of the electric field, drift velocity, and drift times for the smaller drift volumes.

With these basic parameters established, we can now move on to calculating the electric field in the main drift region (between the cathode and the shield plane).

Single line diagram method

The electric field strength in the LArIAT main drift volume can be determined knowing the voltage applied to the cathode, the voltage applied at the shield plane, and the distance between them. We assume the distance between the cathode and the shield plane to be 470 mm and any length contraction due to the liquid argon is negligibly small (∼2 mm).

The voltage applied to the cathode can be calculated using Ohm's law and the single line diagram shown in Figure A.2. A set of two of filter pots for emergency power dissipation are positioned between the Glassman power supply and the cathode, one at each end of the feeder cable, each with an internal resistance of 40 MΩ.

Given the TPC resistor chain, the total TPC impedance is 6 GΩ. Since the total resistance on the circuit is driven by the TPC impedance, we expect the resulting current to be

$$I = V_{PS}/R_{tot} = -23.5 \text{ kV}/6 \text{ G}\Omega \sim 4 \ \mu\text{A}, \tag{A.3}$$

which we measure with the Glassman power supply, shown in Figure A.3.

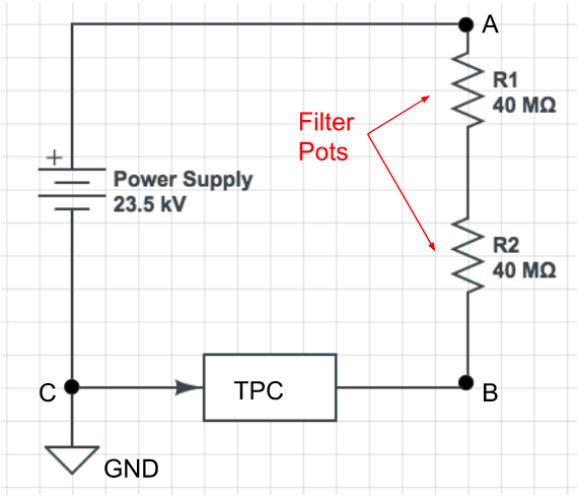

Figure A.2: LArIAT HV simple schematics.

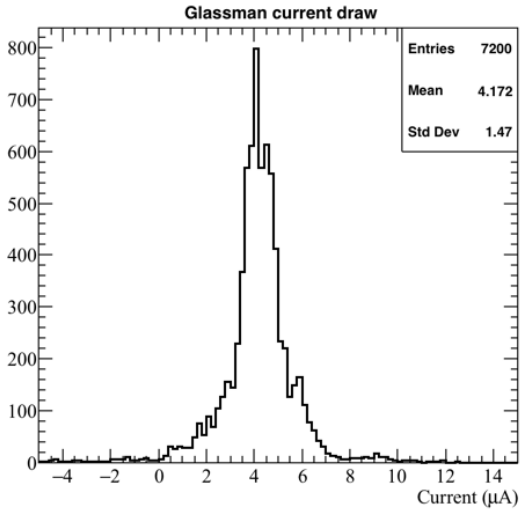

Figure A.3: Current reading from the Glassman between May 25th and May 30th, 2016 (typical Run-II conditions).

Using this current, the voltage at the cathode is calculated as

$$V_{BC} = V_{PS} - (I \times R_{eq}) = -23.5 \text{ kV} + (0.00417 \text{ mA} \times 80 \text{ M}\Omega) = -23.17 \text{ kV}, \quad \text{(A.4)}$$

where I is the current and R_{eq} is the equivalent resistor representing the two filter pots. The electric field is then calculated to be

$$E_{\text{field}} = \frac{V_{BC} - V_{\text{shield}}}{\Delta x} = 486.54 \text{ V/cm}. \quad \text{(A.5)}$$

E field using cathode-anode piercing tracks

We devise an independent method to measure the drift time (and consequently drift velocity and electric field) using TPC cathode to anode piercing tracks. We use this method as a cross check to the single line method. The basic idea is simple:

0. Select cosmic ray events with only 1 reconstructed track
1. Reduce the events to the one containing tracks that cross both anode and cathode
2. Identify the first and last hit of the track
3. Measure the time difference between these two hits (Δt).

This method works under the assumptions that the time it takes for a cosmic particle to cross the chamber ($\sim$ns) is small compared to the charge drift time ($\sim$ hundreds of μs).

We choose cosmic events to allow for a high number of anode to cathode piercing tracks (ACP tracks), rejecting beam events where the particles travel almost perpendicularly to drift direction. We select events with only one reconstructed track to maximize the chance of selecting a single crossing muon (no-michel electron). We utilize ACP tracks because their hits span the full drift length of the TPC, see figure

A.4, allowing us to define where the first and last hit of the tracks are located in space regardless of our assumption of the electric field.

One of the main features of this method is that it doesn't rely on the measurement of the trigger time. Since Δt is the time difference between the first and last hit of a track and we assume the charge started drifting at the same time for both hits, the measurement of the absolute beginning of drift time t_0 is unnecessary. We boost the presence of ACP tracks in the cosmic sample by imposing the following requirements on tracks:

- vertical position (Y) of first and last hits within ± 18 cm from TPC center (avoid Top-Bottom tracks)
- horizontal position (Z) of first and last hits within 2 and 86 cm from TPC front face (avoid through going tracks)
- track length greater than 48 cm (more likely to be crossing)
- angle from the drift direction (phi in figure A.5) smaller than 50 deg (more reliable tracking)
- angle from the beam direction (theta in figure A.5) greater than 50 deg (more reliable tracking)

Tracks passing all these selection requirements are used for the Δt calculation.

For each track passing our selection, we loop through the associated hits to retrieve the timing information. The analysis is performed separately on hits on the collection plane and induction plane, but lead to consistent results. As an example of the time difference, figures A.6 and A.7 represent the difference in time between the last and first hit of the selected tracks for Run-II Positive Polarity sample on the collection and induction plane respectively. We fit with a Gaussian to the peak of the Δt distributions to extract the mean drift time and the uncertainty associated with it.

The long tail at low Δt represents contamination of non-ACP tracks in the track selection. We apply the same procedure to Run-I and Run-II, positive and negative polarity alike.

To convert Δt recorded for the hits on the induction plane to the drift time we employ the formula

$$t_{drift} = \Delta t - t_{S-I} \tag{A.6}$$

where t_{drift} is the time the charge takes to drift in the main volume between the cathode and the shield plane and t_{S-I} is the time it takes for the charge to drift from the shield plane to the induction plane. In Table A.1 we calculated the drift velocity in the S-I region, thus we can calculate t_{S-I} as

$$t_{S-I} = \frac{l_{S-I}}{v_{S-I}} = \frac{4mm}{1.73mm/\mu s} \tag{A.7}$$

where l_{S-I} is the distance between the shield and induction plane and v_{S-I} is the drift velocity in the same region. A completely analogous procedure is followed for the hits on the collection plane, taking into account the time the charge spent in drifting from shield to induction as well as between the induction and collection plane The value for Δt_{drift} , the calculated drift velocity (v_{drift}), and corresponding drift electric field for the various run periods is given in Table A.2 and are consistent with the electric field value calculated with the single line diagram method.

Delta t_{drift}, drift v and E field with ACP tracks

Data Period	Δt_{Drift} [μs]	Drift velocity [mm/μs]	E field [V/cm]
RunI Positive Polarity Induction	311.1 ± 2.4	1.51 ± 0.01	486.6 ± 21
RunI Positive Polarity Collection	310.9 ± 2.6	1.51 ± 0.01	487.2 ± 21
RunII Positive Polarity Induction	315.7 ± 2.8	1.49 ± 0.01	467.9 ± 21
RunII Positive Polarity Collection	315.7 ± 2.7	1.49 ± 0.01	467.9 ± 21
RunII Negative Polarity Induction	315.9 ± 2.6	1.49 ± 0.01	467.1 ± 21
RunII Negative Polarity Collection	315.1 ± 2.8	1.49 ± 0.01	470.3 ± 21
Average Values	314.1	1.50 ± 0.01	474.3 ± 21

Table A.2: Δt for the different data samples used for the Anode-Cathode Piercing tracks study.

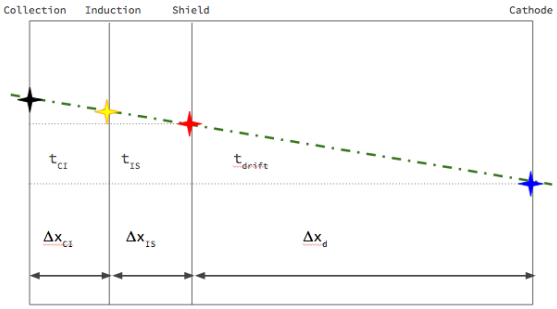

Figure A.4: Pictorial representation of the YX view of the TPC. The distance within the anode planes and between the shield plane and the cathode is purposely out of proportion to illustrate the time difference between hits on collection and induction. An ACP track is shown as an example.

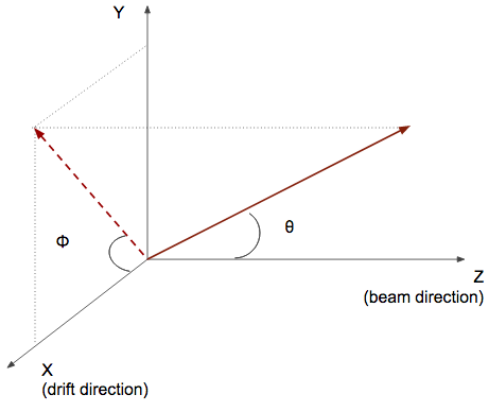

Figure A.5: Angle definition in the context of LArIAT coordinate system.

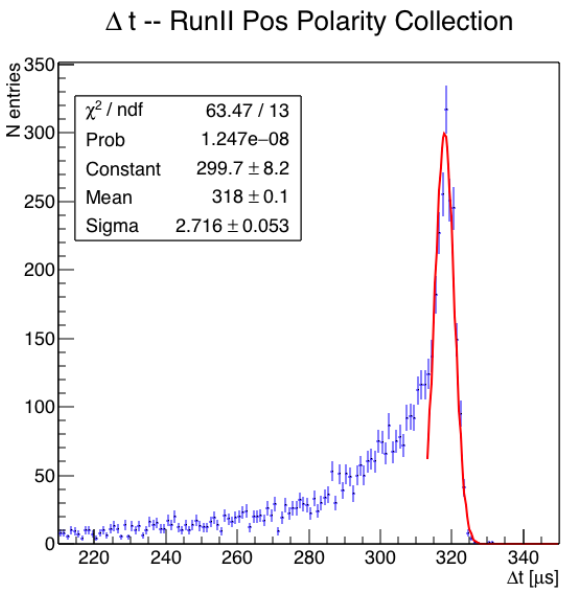

Figure A.6: Collection plane Δt fit for Run II positive polarity ACP data selected tracks.

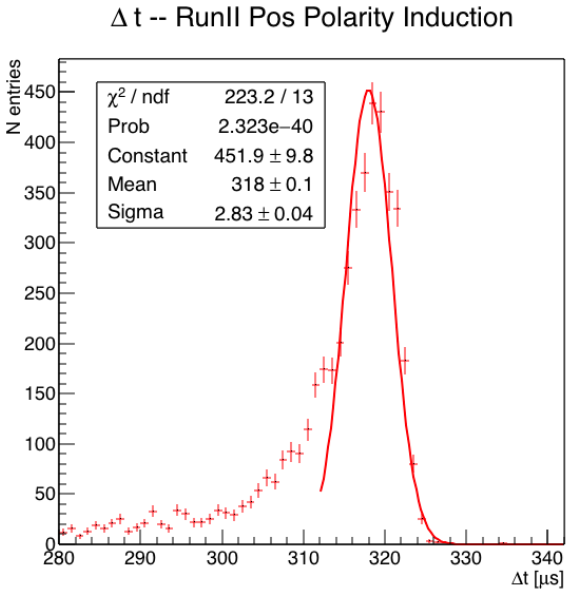

Figure A.7: Induction plane Δt fit for Run II positive polarity ACP data selected tracks.